Grid Connected Dual VSI Modules with Renewable Sources for Power Quality Improvement using Optimal Power Sharing

N. Srilatha[1], V. Jayamadhuri [2]
[1]*Associate Professor, Department of Electrical Engineering, Osmania University*
[2]*PG student, Department of Electrical Engineering, Osmania University*

***Abstract*—In this paper dual VSI modules are introduced into a 3-ph grid with unbalanced linear and non-linear loads. One of the VSI (Voltage Source Inverter) modules is connected with a DC source operating as DG (Distributed Generation) unit and the other VSI module is connected with capacitor operating as STATCOM (Static Synchronous Compensator). The DG module VSI compensates the active power of the load and the STATCOM-VSI module compensates the reactive power and harmonics introduced by the non-linear load. Both the modules are operated with ISCT (Instantaneous Symmetrical Component Theory) control structure for synchronized power sharing. The DG-VSI module is later updated with renewable source like PV (Photo Voltaic) along with BESS (Battery Energy Storage System) replacing conventional DC source. An active power control and DC link voltage control are integrated to control DG-VSI and STATCOM-VSI modules respectively. Active and reactive power comparison graphs are shown, achieving renewable power sharing, reactive power and harmonics compensation.**

***Index Terms*— BESS (Battery Energy Storage System), DG (Distributed Generation), ISCT (Instantaneous Symmetrical Component Theory), STATCOM (Static Synchronous Compensator), VSI (Voltage Source Inverter).**

I. INTRODUCTION

With increase in power demand on the electrical power grid more generation is required which needs to be renewable power. Most of the DG (Distributed Generation) units [1] in the grid are renewable power sources like PV (Photo Voltaic), wind farm, fuel cell, bio-gas units. The conventional power generation is replaced with these DG units for renewable power sharing to the grid. To achieve this, power electronic devices are introduced for the conversion of power and sharing to the grid in synchronization. These power electronic modules convert DC power generated by the PV or fuel cell sources to 3-ph AC voltages and share their power to the grid. As these sources are connected in parallel to the grid the load power is compensated mostly by these renewable DG units, reducing the consumption from the conventional fossil fuel source [2]. Along with this major power quality issues in a grid like harmonics, drop in power factor or voltage fluctuations can also be solved [3]. Therefore, to mitigate the mentioned power quality issues, dual VSI (Voltage Source Inverter) modules [3] are introduced into the 3-ph grid. One of the VSI modules is considered to be renewable source DG module and the other is considered as STATCOM (Static Synchronous Compensator) device. The DG-VSI module is connected with 6-IGBT switches (S_{ma}, S'_{ma}, S_{mb}, S'_{mb} S_{mc} and S'_{mc}) and PV renewable source on the DC side of the module. Along with PV source a BESS (Battery Energy Storage System) unit is also connected in parallel to the PV unit for power stability [4]. In the second VSI module the same 6-switch IGBT (S_{xa}, S'_{xa}, S_{xb}, S'_{xb} S_{xc} and S'_{xc}) circuit is connected to an ultra-capacitor on the DC side. The DG-VSI module shares only active power to the grid, whereas the capacitor VSI module shares reactive power and also mitigates harmonics (induced by non-linear load) in the grid. The complete circuit structure of the proposed system with dual VSI can be seen in Fig. 1.
As observed in Fig. 1, both the VSI modules [5] are connected at PCC (Point of Common Coupling) where powers are shared and also harmonics mitigation can be achieved. Both the VSI modules are operated by ISCT control structure [6] with feedback taken from PCC voltages (Vt_{abc}) and load currents (Il_{abc}). Each module is connected with inductive filters (L_f) for mitigation of harmonics introduced by the VSI modules. The DG-VSI module is connected with PV

unit which is included with boost converter and MPPT (Maximum Power Point Algorithm) control [10]. For reduction of complexity, simple P&O MPPT algorithm is used to operate the boost converter [11]. Along with PV unit a BESS unit [12] is also connected in parallel to the PV unit for power sharing during lower solar irradiation or higher power demand conditions.

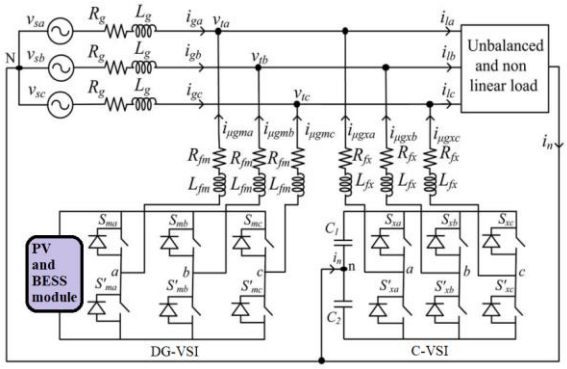

Fig. 1: Proposed Dual VSI integrated system

II. PROPOSED TOPOLOGY

As seen in Fig. 1, the 3-ph grid is connected with unbalanced linear and non-linear loads. Here V_{sa} V_{sb} and V_{sc} are the 3-ph grid voltages with grid impedance R_g and L_g. At the PCC, 3-ph grid source, unbalanced loads and dual VSI modules are connected. The voltages at PCC are defined as V_{ta} V_{tb} and V_{tc} which are the 3-ph voltages common for all the modules. All the modules need to be synchronized to these PCC voltages in order to share powers. Here the DG-VSI module injects currents $i_{\mu gma}$, $i_{\mu gmb}$ and $i_{\mu gmc}$ which are the active power currents. The C-VSI injects reactive power and harmonics compensation currents $i_{\mu gxa}$, $i_{\mu gxb}$ and $i_{\mu gxc}$ at PCC [7]. The DC link side of C-VSI is connected with two ultra capacitors (C_1 and C_2) connected by neutral point. The capacitor current consumption [5] provides reactive power to the grid. The reactive power compensation depends on reference DC voltage ($V_{dc\ ref}$) in the ISCT controller [3]. The value of the DC link side capacitors are taken as

$$C_1 = C_2 = \frac{2nST}{V_{dcr}^2 - V_{dc1}^2} \quad (1)$$

Here, n is the voltages controller number of cycles taken as 1, S is the load apparent power rating, T is the sample time, V_{dcr} is 520V and V_{dc1} is minimum voltage allowable which is 0.8*V_{dcr}. The filter inductance of C-VSI and DG-VSI is calculated as

$$L_{fx} = \frac{1.6V_m}{4h_x f_{max}} \quad (2)$$

Here, V_m is maximum phase voltage, h_x is hysteresis band (2%), f_{max} is maximum switching frequency.

On the DC link side of DG-VSI the conventional DC source is replaced with renewable PV source [4] generating DC power from natural source solar irradiation. As it is estimated that solar irradiation is not constant throughout a day the power from PV source varies which impacts the voltage. Therefore a DC-DC boost converter is connected to the PV module which boosts the voltage of PV to higher amplitude. The boost converter extracts maximum power from PV source which is controlled by MPPT algorithm control [10]. P&O (Perturb and Observe) MPPT technique is adopted for the control of the boost converter. The P&O MPPT [11] takes feedback from PV source voltage (V_{pv}) and current (I_{pv}) which generates the required duty ratio for the boost converter extracting maximum power. The P&O MPPT operating flow chart can be seen in Fig. 2.

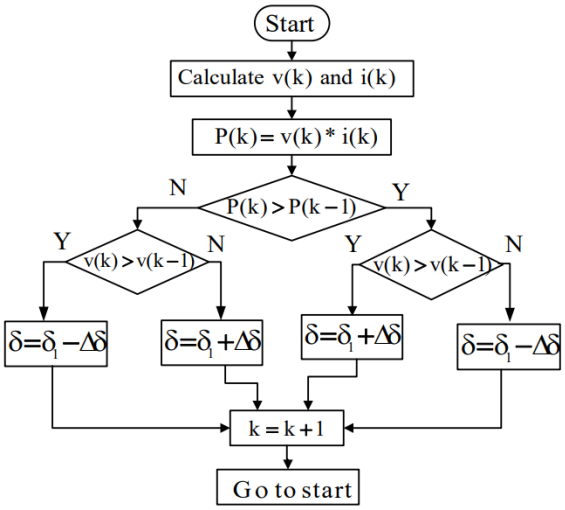

Fig. 2: Conventional P&O MPPT flow chart

As per the give flow chart in Fig. 2 the duty ratio (δ) for the boost converter control is generated as per the given comparison conditions below.

If P(k) > P(k-1) and V(k) > V(k-1) then $\delta = \delta_1 + \Delta\delta$
If P(k) > P(k-1) and V(k) < V(k-1) then $\delta = \delta_1 - \Delta\delta$
If P(k) < P(k-1) and V(k) > V(k-1) then $\delta = \delta_1 - \Delta\delta$
If P(k) < P(k-1) and V(k) < V(k-1) then $\delta = \delta_1 + \Delta\delta$

Here, P(k), V(k) are the present values and P(k-1), V(k-1) are the past values of PV source power and voltage respectively [11]. The $\Delta\delta$ value is the update to the past value of duty ratio δ_1 which either increases

or decreases the present δ value as per the given conditions.

The power of PV source fluctuates with respect to solar irradiation, where the power can be excess or deficit as per the required demand. Therefore, the PV source is connected in parallel with BESS unit [12] which stores or provides power during excess or deficit PV power conditions respectively. For these operating conditions the battery pack is connected to bidirectional converter with two operating switches (Q1 and Q2). The bidirectional converter [13] is controlled by constant voltage (CV) control which operates with certain reference voltage (V_{dc}^*). The boost converter of PV source also tends to operate at the given V_{dc}^* value given in CV controller. The below Fig. 3 is the renewable source unit which is connected at the DC link of DG-VSI.

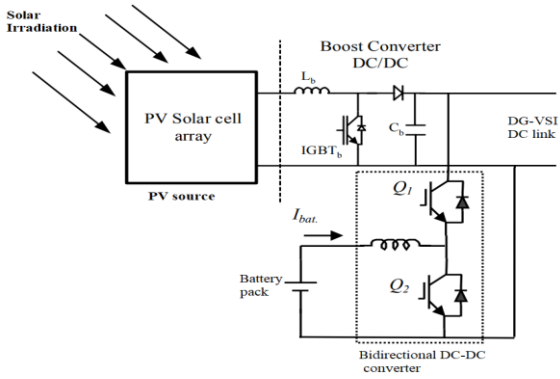

Fig. 3: PV and BESS module

In the bidirectional DC-DC converter the Q1 and Q2 switches are operated alternatively. The duty ratios of the switches are adjusted as per the required operating condition (charge or discharge). The variable duty ratio for the switches is generated by CV control in which a conventional PI controller is used [13]. The CV control for operating the bidirectional DC-DC converter is shown in Fig. 4.

III. DUAL VSI CONTROLLER MODULE

For the control of both VSI modules ISCT controller [14] is integrated with reference voltage ($V_{dc\,ref}$) for the C-VSI and reference active power ($P_{\mu g}$) for the DG-VSI. The controller takes input from PCC voltages (V_{tabc}) and load currents (I_{labc}) generating reference signals for the hysteresis current loop controller. The complete control structure of ISCT with internal modules can be seen in Fig. 5.

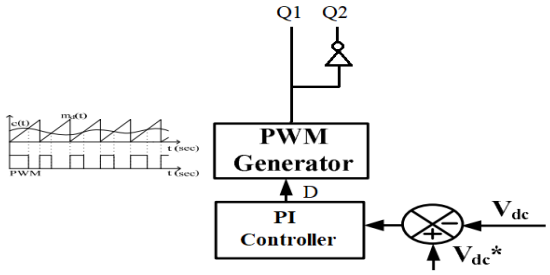

Fig. 4: CV control with reference DC voltage V_{dc}^*

For the generation of DG-VSI reference currents ($i^*_{\mu gm\,(abc)}$) reference active power ($P_{\mu g}$) and filtered PCC voltages ($V^+_{t1(abc)}$) are considered [3]. The filtering of the PCC voltages is achieved by moving average filter which is low pass filter (LPF) with fundamental frequency 15Hz. The filtering process is included with Park's and Inverse Park's transformation as given below.

$$\begin{bmatrix} V_{td} \\ V_{tq} \end{bmatrix} = \begin{bmatrix} Sin\,\theta & -Cos\theta & 0 \\ Cos\theta & Sin\theta & 0 \end{bmatrix} \begin{bmatrix} V_{ta} \\ V_{tb} \\ V_{tc} \end{bmatrix} \quad (3)$$

The dq voltage components are filtered for reduction of disturbances in the signals with LPF, generating $\overline{V_{td}}$ and $\overline{V_{tq}}$. The filtered dq components are converted back to V^+_{t1abc} signals using the below conversion.

$$\begin{bmatrix} V^+_{t1a} \\ V^+_{t1b} \\ V^+_{t1c} \end{bmatrix} = \begin{bmatrix} Sin\theta & Cos\theta \\ Sin\left(\theta - \frac{2\pi}{3}\right) & Cos\left(\theta - \frac{2\pi}{3}\right) \\ Sin\left(\theta + \frac{2\pi}{3}\right) & Cos\left(\theta + \frac{2\pi}{3}\right) \end{bmatrix} \begin{bmatrix} \overline{V_{td}} \\ \overline{V_{tq}} \end{bmatrix} \quad (4)$$

With the above signals the DG-VSI reference ($i^*_{\mu gm\,(abc)}$) is given as

$$i^*_{\mu gm\,(abc)} = P_{\mu g} \left(\frac{V^+_{t1\,(abc)}}{(V^+_{ta})^2 + (V^+_{tb})^2 + (V^+_{tc})^2} \right) \quad (5)$$

These reference currents of DG-VSI ($i^*_{\mu gm\,(abc)}$) are compared to measured currents and the error is fed to hysteresis band [15] generating pulses for VSI switches.

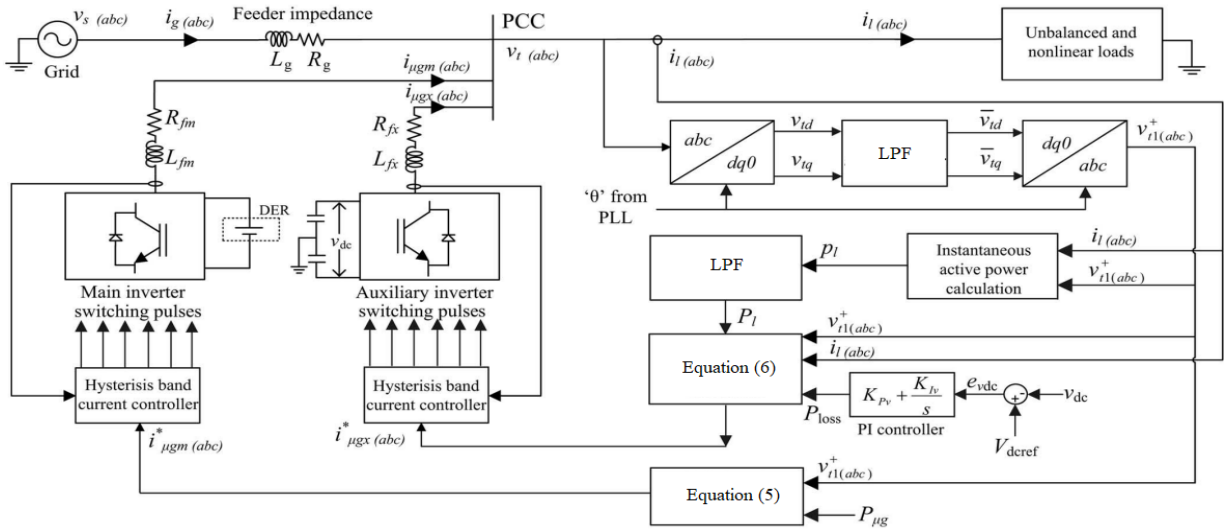

Fig. 5: ISCT control for Dual VSI modules

The reference current of C-VSI for phase a is generated as given below.

$$i^*_{\mu gx\,(abc)} = \left(\frac{V^+_{t1\,(abc)}}{(V^+_{ta})^2 + (V^+_{tb})^2 + (V^+_{tc})^2}\right)(P_l + P_{loss} - P_{\mu g}) \quad (6)$$

In the above equation P_l is the measured active power requirement of load and P_{loss} is calculated with comparison of DC link voltage given as

$$P_{loss} = (V_{dc\,ref} - V_{dc})(K_p + \int K_i\,.\,dt) \quad (7)$$

Here, Kp and Ki are the proportional and integral gains of PI controller which are tuned as per the response of the C-VSI module measured DC link voltage (V_{dc}). The reference currents $i^*_{\mu gx\,(abc)}$ are now compared to measured C-VSI currents ($i_{\mu gx\,(abc)}$) generating error which is fed to hysteresis band controlling the switches. These modules are modeled and the results are generated with comparative analysis in next section IV.

IV. SIMULATION RESULTS

The test system with 3-ph grid, unbalanced non-linear loads and dual VSI modules is modeled with certain ratings similar to actual grid parameters. The below TABLE I are the parameters considered for the modeling of the test system.

With these parameters all the modules are modeled in MATLAB Simulink environment with different operating conditions. These changes in operating conditions determine performance of the dual VSI modules. All the graphs are generated using powergui toolbox with respect to time.

TABLE I: SIMULATION SYSTEM PARAMETERS

Name of the parameter	Value
Grid rating	440Vrms, 50Hz, Rg=0.5Ω, Lg=1mH.
DG-VSI parameters	DC link voltage V_{dcm} = 700V, Filter impedance R_{fm} = 0.25Ω, L_{fm} =5mH, Hysteresis limits = ±0.2A.
Renewable source modules	*PV parameters* V_{mp} = 54.7, I_{mp} = 5.58A, V_{oc}=64.2V, I_{sc}=5.96A, N_s=7, N_p=3, P_{pv} = 6.4kW. *Battery parameters* V_{bat}=350V, Capacity=40Ah. *Boost converter* L_b=5mH, C_{in}=100µF, C_{out}=12000µF. *Bidirectional converter* L_{bc}=1mH, C_{in}=220µF, C_{out}=2200µF.
C-VSI parameters	C1=C2=2200µF, Vdc ref = 1040V, Filter impedance R_{fx}=0.25, L_{fx}=20mH, Hysteresis limits = ±0.2A.
Linear load	Z_{la}=30+j20Ω Z_{lb}=32+j15Ω Z_{lc}=25+j15Ω
Non-liner load	Diode bridge rectifier connected to R_{load} = 188Ω
Bidirectional controller gains	$K_{p\,bat}$ = 0.15, $K_{i\,bat}$ = 0.5
ISCT DC voltage controller gains	$K_{p\,dc}$ = 10, $K_{i\,dc}$ = 0.05
LPF frequency	15Hz

The total simulation time considered is 1sec in which the dual VSI modules are connected at 0.2sec. The total load power demand is set to be 6kW and 2.3kVAR and the controller reference power is set 5kW. The condition from 0.2sec is grid sharing condition where the grid and VSI modules share power to load. This reference power is changed to 7kW at 0.7sec injecting more power changing the state to grid injecting condition. As per the given conditions the graphs of different measurements are shown below.

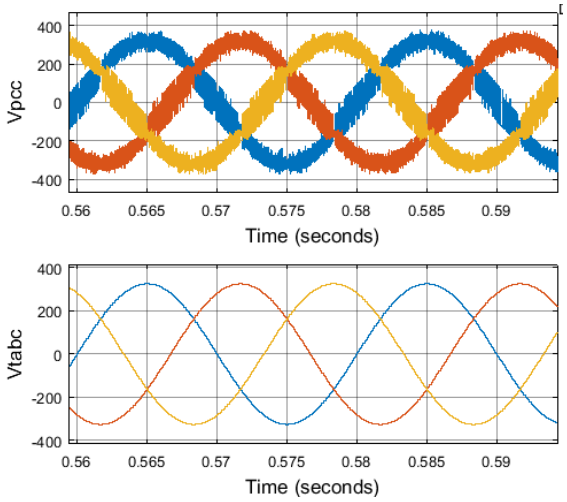

Fig. 6: 3-ph PCC voltages and filtered voltages

The above Fig. 6, the 3-ph PCC voltages and the LPF filtered voltages are shown. As seen the disturbances in the signals are reduced making it pure sinusoidal waveform which is used in the ISCT controller.

In the graph of Fig. 7, the first axis is load current which are unbalanced as per the given value in TABLE 1. The second axis is the grid currents which are reduced and balanced once the Dual VSI modules are connected at 0.2sec. The third axis is the DG-VSI currents which are injected from 0.2sec and are increased at 0.7sec as per the conditions given. The C-VSI currents are shown in fourth axis which compensate reactive power and harmonics of the source. As per the given conditions Fig. 8 is the power factor of the grid source which change from 0.93 to 0.99 at 0.2sec. The power factor is changed to -0.99 at 0.7sec when the condition is changed from grid sharing to grid injected mode.

As observed in Fig. 9 graph the first axis is the load power which is always at 6kW irrespective of any changes in the system. The second axis is the grid power which dropped from 6kW to 1kW when Dual VSI modules are connected. At 0.7sec the power changes to -1kW denoting grid injection from DG-VSI as the power reference in ISCT is changed from 5kW to 7kW which can be seen in third axis. The last fourth axis is the active power of C-VSI module which is maintained at 0 in any given condition.

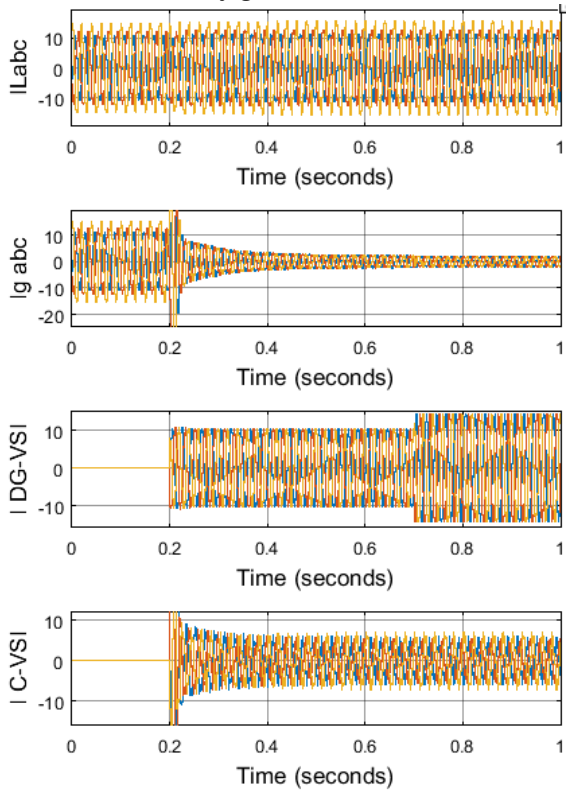

Fig. 7: 3-ph currents of load, grid, DG-VSI, C-VSI

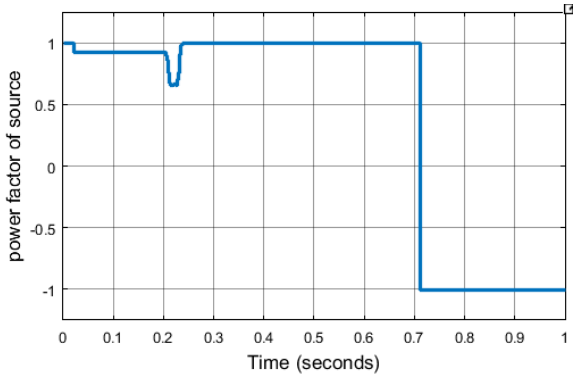

Fig. 8: Power factor of the 3-ph grid source

In the below Fig. 10 the first axis is the load reactive power noted at 2.3kVAR and the second axis is the compensation reactive power provided by the C-VSI

module. The third axis is the DG-VSI module reactive power which is always 0 in any given condition.

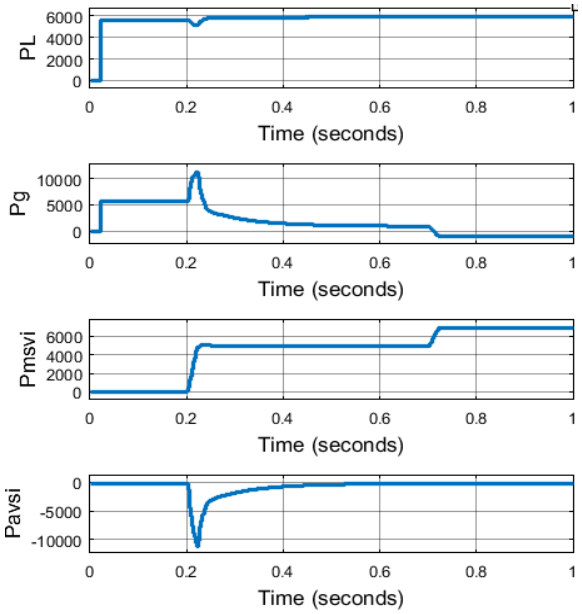

Fig. 9: Active powers of load, grid, DG-VSI, C-VSI

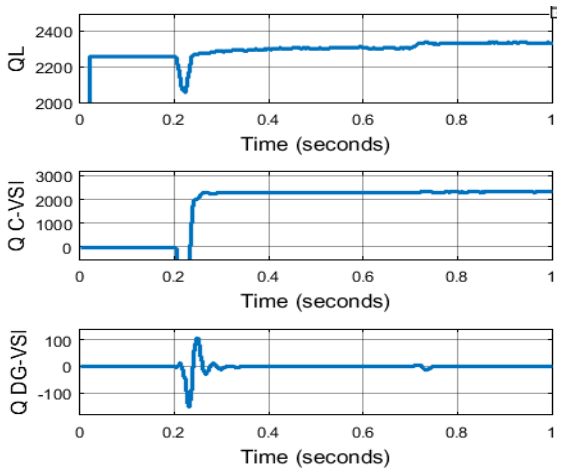

Fig. 10: Reactive powers of load, C-VSI, DG-VSI

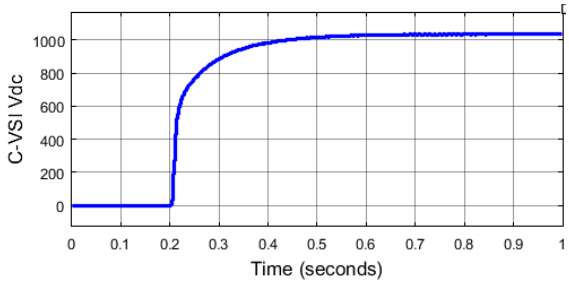

Fig. 11: DC link voltage of C-VSI module

The above Fig. 11 is the DC link voltage of C-VSI module which is settled at 1040V rising from 0.2sec. The value is given as reference as per table 1 in ISCT controller. As per the given conditions the below Fig. 12 are the powers of PV source and battery unit. As observed initially at 0sec the PV power generated is 6kW and it remained same as the solar irradiation is maintained at 1000W/mt^2 throughout the simulation.

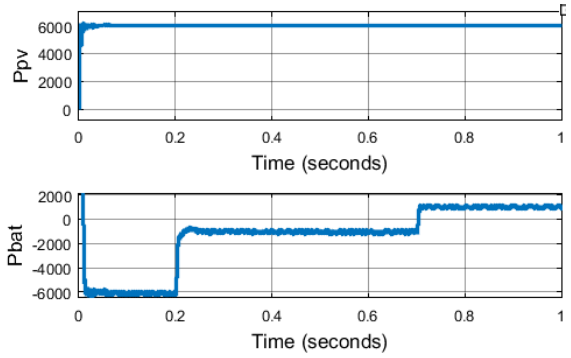

Fig. 12: PV source and Battery powers

The battery power at 0 sec is -6kW which indicates charging of the battery with total PV power as the Dual VSI modules are disconnected from 3-ph grid. At 0.2sec when the Dual VSI modules are connected to grid the charging power of battery is dropped to –1kW as 5kW is shared to the load. At 0.7sec when the reference power is changed to 7kW the battery power is changed to 1kW making it to discharge supporting the load and injecting the remaining power back to grid. The below Fig. 13 is the phase A PCC voltage and grid current which are in phase until 0.7sec and 180degree phase shift after 0.7sec.

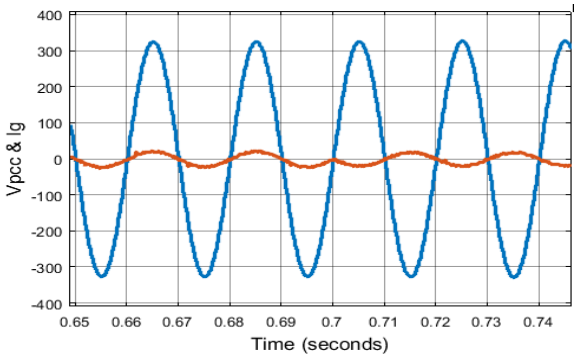

Fig. 13: Phase A PCC voltage and grid current

The below Fig. 14 is the phase A PCC voltage and DG-VSI current which are always in phase before and after 0.7sec.

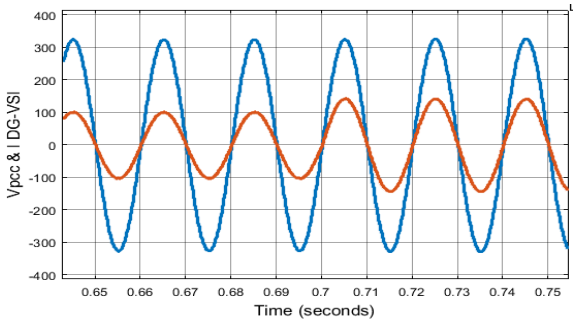

Fig. 14: Phase A PCC voltage and DG-VSI current

FFT analysis is carried out on phase A grid current determining the Total Harmonic Distortion (THD) is shown in Fig. 14 before connecting Dual VSI modules, followed by Fig. 15 which is FFT analysis of the same after connecting Dual VSI modules.

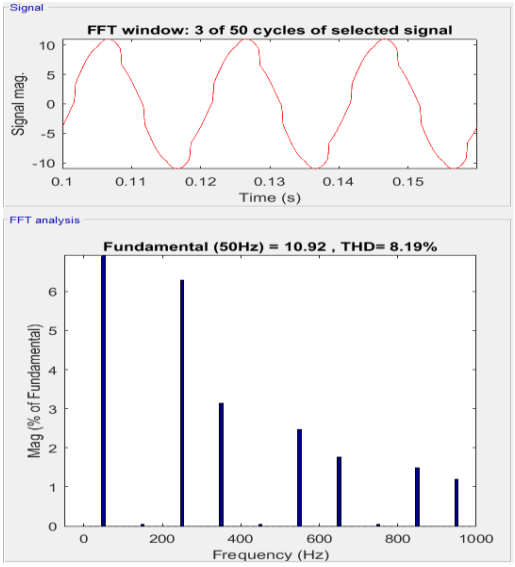

Fig. 15: THD before connecting Dual VSI modules

The final discussion and parametric comparison of different parameters is given in next section. The tabular comparison of the various parameters in different time zones is summarized in Table II.

TABLE II: PARAMETRIC COMPARISON

	0-0.2sec	**0.2-0.7sec**	**0.7-1sec**
P_{grid}	6kW	1kW	-1kW
Q_{grid}	2.3kVAR	0kVAR	0kVAR
Grid power factor	0.93	0.99	-0.99
THD of I_{ga}	8.19%	5.09%	5.09%

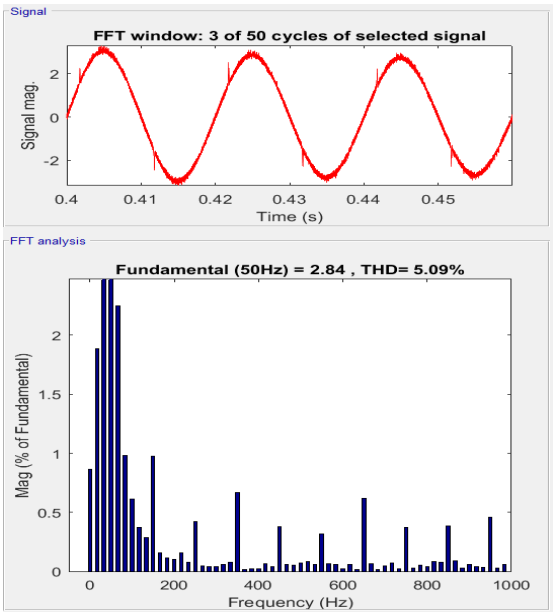

Fig. 16: THD after connecting Dual VSI modules

VII. CONCLUSION

Successful implementation of given test system with operating conditions changed showing the performance of Dual VSI modules is done. It is also proved that these VSI modules are improving the power quality of the grid with reduced THD and also share renewable power to the load. Both active and reactive powers of the load are completely compensated by the DG-VSI and C-VSI modules respectively. With change in reference power value the extra power is also injected back to grid. The power factor of the source is also improved maintained at unity after connecting the Dual VSI modules. The below table II is the final parametric comparison as per the change in conditions of 1sec simulation time.

REFERENCES

[1] P. A. Souza, G. B. D. Santos, V. Mariano and D. Barbosa, "Analysis of active and reactive power injection in distributed systems with photovoltaic generation," 2018 Simposio Brasileiro de Sistemas Eletricos (SBSE), 2018, pp. 1-6.

[2] J. Chauhan and B. S. Surjan, "Impact of Distributed Generation in Single area load frequency control on system frequency," 2020 IEEE International Students' Conference on Electrical, Electronics and Computer Science (SCEECS), 2020, pp. 1-5.

[3] M. V. Manoj Kumar, M. K. Mishra and C. Kumar, "A Grid-Connected Dual Voltage Source Inverter With Power Quality Improvement Features," in IEEE Transactions on Sustainable Energy, vol. 6, no. 2, pp. 482-490, April 2015.

[4] X. Li, L. Wang, N. Yan and R. Ma, "Cooperative Dispatch of Distributed Energy Storage in Distribution Network With PV Generation Systems," in IEEE Transactions on Applied Superconductivity, vol. 31, no. 8, pp. 1-4, Nov. 2021, Art no. 0604304.

[5] J. Lee, M. -W. Kim, I. Kim and J. -W. Park, "Analysis of DC-Link Voltage Ripple by Generalized Discontinuous PWM Strategy in Two-Level Three-Phase Voltage Source Inverters," 2022 IEEE Transportation Electrification Conference & Expo (ITEC), 2022, pp. 49-54.

[6] S. Jahan, S. P. Biswas, S. Haq, M. R. Islam, M. A. P. Mahmud and A. Z. Kouzani, "An Advanced Control Scheme for Voltage Source Inverter Based Grid-Tied PV Systems," in IEEE Transactions on Applied Superconductivity, vol. 31, no. 8, pp. 1-5, Nov. 2021, Art no. 5401705.

[7] A. Abdelhakim, F. Blaabjerg and P. Mattavelli, "Modulation Schemes of the Three-Phase Impedance Source Inverters—Part I: Classification and Review," in IEEE Transactions on Industrial Electronics, vol. 65, no. 8, pp. 6309-6320, Aug. 2018

[8] K. Luo and W. Shi, "Comparison of Voltage Control by Inverters for Improving the PV Penetration in Low Voltage Networks," in IEEE Access, vol. 8, pp. 161488-161497, 2020

[9] J. P. Bonaldo, J. d. A. Olímpio Filho, A. M. dos Santos Alonso, H. K. Morales Paredes and F. Pinhabel Marafão, "Modeling and Control of a Single-Phase Grid-Connected Inverter with LCL Filter," in IEEE Latin America Transactions, vol. 19, no. 02, pp. 250-259, February 2021.

[10] D. Jiandong, X. Ma and S. Tuo, "A Variable Step Size P&O MPPT Algorithm for Three-Phase Grid-Connected PV Systems," 2018 China International Conference on Electricity Distribution (CICED), 2018, pp. 1997-2001.

[11] M. H. Reza and M. A. Shobug, "Efficiency Evaluation of P&O MPPT Technique used for Maximum Power Extraction from Solar Photovoltaic System," 2020 IEEE Region 10 Symposium (TENSYMP), 2020, pp. 1808-1811.

[12] O. M. Akeyo, V. Rallabandi, N. Jewell and D. M. Ionel, "The Design and Analysis of Large Solar PV Farm Configurations With DC-Connected Battery Systems," in IEEE Transactions on Industry Applications, vol. 56, no. 3, pp. 2903-2912, May-June 2020.

[13] Y. Yang, Q. Ye, L. J. Tung, M. Greenleaf and H. Li, "Integrated Size and Energy Management Design of Battery Storage to Enhance Grid Integration of Large-Scale PV Power Plants," in IEEE Transactions on Industrial Electronics, vol. 65, no. 1, pp. 394-402, Jan. 2018.

[14] P. Gharde, N. Pande and P. D. Debre, "Load compensation of a stiff system using ISCT based D-STATCOM under unbalanced and non-linear load condition," 2017 International Conference on Innovations in Information, Embedded and Communication Systems (ICIIECS), 2017, pp. 1-4.

[15] M. Kumar, N. Gupta and R. Garg, "Unity power factor control of grid connected SPV system using instantaneous symmetrical component theory," 2016 IEEE 1st International Conference on Power Electronics, Intelligent Control and Energy Systems (ICPEICES), 2016, pp. 1-6.